RSC Sustainability

ROYAL SOCIETY OF CHEMISTRY

PAPER

View Article Online
View Journal | View Issue

Cite this: *RSC Sustainability*, 2025, **3**, 1003

From lead–acid batteries to perovskite solar cells – efficient recycling of Pb-containing materials†

Jiajia Suo, *[ab] Bowen Yang, [a] Sonja Prideaux,[b] Henrik Pettersson[b] and Lars Kloo [c]

The most efficient and stable perovskite solar cells typically contain lead compounds as a key component in the light-absorbing layer. To advance the commercialization of perovskite photovoltaics, it is crucial to address sustainability concerns regarding the use of toxic lead. In this work, we have developed a straightforward lead recycling pathway that converts lead compounds from lead–acid batteries into lead iodide. Purity analyses of the resulting lead iodide and the direct fabrication of perovskite solar cells demonstrate that the recycled lead iodide matches the quality of commercially available products. Most importantly, establishing this efficient lead recycling process not only supports sustainable recycling and resource utilization in a circular materials flow but also promotes the future development of perovskite photovoltaics.

Received 13th August 2024
Accepted 24th December 2024

DOI: 10.1039/d4su00470a

rsc.li/rscsus

Sustainability spotlight

Lead compounds are critical for fabricating efficient perovskite solar cells (PSCs), despite their toxicity. Rather than exploring new lead sources, it is crucial to develop efficient recycling pathways for lead from waste products to minimize waste generation as well as protect both the environment and human health. In this work, we have established a straightforward lead recycling method using widely available lead–acid batteries to produce lead iodide, a key component in the light-absorbing layer of PSCs. Our work aligns with the UN Sustainable Development Goal (SDG) 12: Responsible Consumption and Production by minimizing waste and improving resource efficiency. Moreover, by advancing the sustainable development of renewable energy technologies, this work contributes to the SDG 7: Affordable and Clean Energy.

Introduction

Perovskite solar cells (PSCs) have emerged as one of the most promising technologies of the next-generation photovoltaics (PVs) due to their excellent device performance, unique defect tolerance, straightforward fabrication process, low manufacturing costs, and other advantages.[1–6] Over the past decade, advancements in materials and device engineering have significantly improved the efficiency and stability of PSCs. Recently, single-junction PSCs have shown power conversion efficiencies (PCEs) exceeding 26%.[7–9] Additionally, the stability of PSCs has markedly improved, with devices passing different industry standard tests, such as the damp heat test (85% relative humidity, 85 °C) and the temperature cycling test (−40 to 85 °C).[10–12] These accomplishments have brought the perovskite PV technology closer to commercialization.[2,13,14]

In perovskite PVs, toxic lead compounds are key components of the light-absorbing materials, playing a crucial role in the generation of highly efficient PSCs. For instance, producing one gigawatt of solar PV capacity with perovskite modules at 20% efficiency would require approximately 3.5 tons of lead, based on a perovskite film thickness of 500 nm. Extrapolating to a broader context, if perovskite photovoltaics would comprise 20% of the anticipated 8500 gigawatt PV market by 2050, the total lead content in these modules could amount to about 6000 tons.[15] To realize future commercialization, exploring new lead resource for perovskite PVs is highly demanded.[16] In industry, extracting lead from ores such as galena, cerussite, and anglesite typically involves multiple steps including mining, crushing, roasting, smelting, and refining.[17] These traditional extraction processes demand high energy input and generate substantial waste products. In addition, these industrial activities produce different pollutants, such as sulfur dioxide (SO_2) and lead-containing dust, leading to significant environmental and health concerns. Therefore, the identification of alternative lead sources for PSCs is highly necessary. This also offers the possibility to make a conceptual change in the materials flow of lead-containing compounds, from a linear flow generating large

[a]*Department of Chemistry, Ångström Laboratory, Uppsala University, SE-75120 Uppsala, Sweden*

[b]*Dyenamo AB, Greenhouse Labs, Teknikringen 38A, SE-114 28 Stockholm, Sweden. E-mail: jiajia.suo@dyenamo.se*

[c]*Department of Chemistry, Applied Physical Chemistry, KTH Royal Institute of Technology, SE-100 44 Stockholm, Sweden*

† Electronic supplementary information (ESI) available. See DOI: https://doi.org/10.1039/d4su00470a

amounts of waste products to a circular flow with minimal waste generation. Recycling lead compounds from used lead–acid batteries to manufacture PSCs offers a promising solution to this challenge. In a lead–acid battery, highly pure lead chemicals (lead and lead dioxide) as well as sulfuric acid (H_2SO_4) requiring a purity of at least 99.9%, are crucial for the performance, longevity, and safety of the batteries. Lead–acid batteries are widely used in a multitude of applications, such as automotive, uninterruptible power supplies, and backup power systems. To avoid environmental pollution and health hazards, over 95% of lead–acid batteries in the world are recycled to fabricate new batteries. In some regions, especially in Europe, the recycling yield is over 99%. However, the growth in lead–acid battery demand may be moderated with the development of competing and superior lithium-ion and other advanced battery technologies, as well as the widespread PV materials. Therefore, the current lead recycling process for manufacturing new lead–acid batteries might be disrupted in the future, necessitating the exploration of alternative reuse pathways.[18–20] With the expected future commercialization of perovskite PVs, using recycled lead materials from the surplus of "end-of-life" lead–acid batteries to produce perovskite PVs offers an ideal solution. Furthermore, the establishment of this new approach will not only reduce the potential environmental impact of industrial activities by developing an alternative lead source but also promote the widespread application of perovskite PVs.

Although some recycling studies have been reported, most of previous studies involve high-temperature calcination (above 500 °C), which require a significant energy input.[17–19] In addition, the use of hazardous chemicals, such as hydrogen peroxide, limits the industrial application of the recycling processes suggested.[20] In this study, we have developed a simple and efficient recycling method suitable for future industrial use. The current process integrates lead compounds, including lead dioxide, lead, lead sulfate, and other mixed lead-based materials, collected from both the positive and negative electrodes of lead–acid batteries. These recycled lead compounds are utilized to synthesize lead iodide (PbI_2), a crucial material for efficient and stable PSCs, as summarized in Fig. 1a. Different purity analysis techniques confirm that the composition of the recycled PbI_2 is similar to that of commercially available PbI_2. Importantly, perovskite devices fabricated based on the recycled PbI_2 following the procedures outlined in this work show comparable performance to those made from commercial PbI_2. This indicates that the recycled PbI_2 meets the high purity standards required for PSCs and matches the quality of commercially available PbI_2.

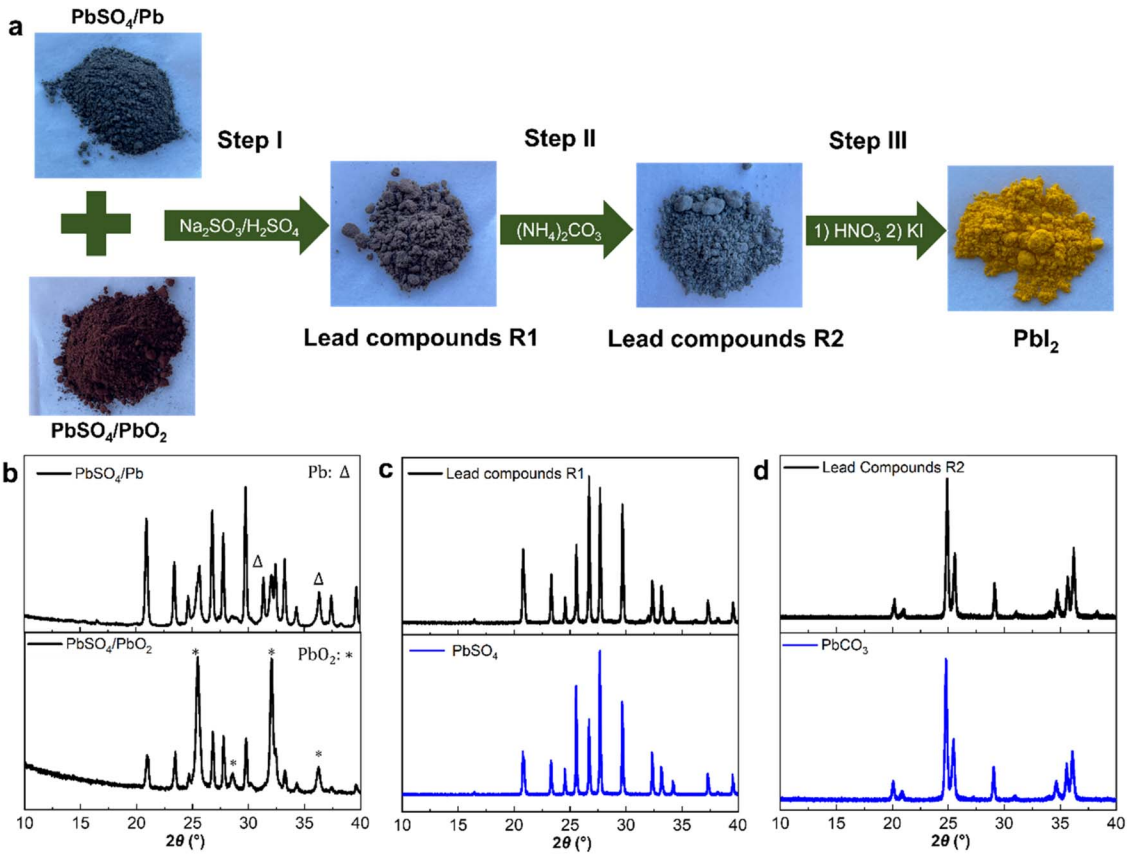

Fig. 1 (a) Lead recycling process from lead–acid battery to PbI_2; (b) XRD patterns of lead-containing compounds from the negative and positive electrodes; (c) XRD patterns of pure $PbSO_4$ and lead-containing compounds after the first step; (d) XRD patterns of pure $PbCO_3$ and lead-containing compounds after the second step.

Results and discussions

Lead recycling process

Ideally, during the discharging process of lead–acid batteries, the lead dioxide (PbO_2) from the positive electrode (cathode) and the lead (Pb) from the negative electrode (anode) both convert to lead sulfate ($PbSO_4$). When the battery is recharged, the lead sulfate on the electrodes reverts back to lead and lead dioxide, respectively. Thus, Pb, PbO_2, and $PbSO_4$ are the primary lead compounds in a lead–acid battery, although different Pb-containing compounds will accumulate during ageing of the battery. To investigate the recycling methods for these three compounds, we discharged a lead–acid battery from 12 V to 5 V, as depicted in Fig. S1.† After disassembling the battery, we collected the lead-containing compounds from the negative and positive electrodes separately. X-ray diffraction (XRD) measurements were then used to confirm the main chemical composition of the lead-based compounds.

As depicted in Fig. 1b and S2,† when comparing the XRD patterns of pure $PbSO_4$ (peaks at 2θ 31.4° and 36.4°) suggest the presence of lead metal in combination with $PbSO_4$ originating from the negative electrode. Meanwhile, 2θ peaks detected at 25.5°, 28.5°, 32.0° and 36.2° indicate a mixture of $PbSO_4$ and PbO_2 within the lead-containing compounds collected from the positive electrode. In order to streamline the recycling process, we mixed the lead-based compounds from both the positive and negative electrodes for subsequent treatment. Sodium sulfite (Na_2SO_3) was used as the reducing agent under acidic (H_2SO_4) conditions to facilitate the reduction of Pb(IV) in PbO_2 to Pb(II) compounds. According to the following reaction (1), PbO_2 reacts with Na_2SO_3 to yield lead oxide (PbO), which promptly undergoes a reaction with H_2SO_4 to form $PbSO_4$. Simultaneously, lead reacts slowly with dilute H_2SO_4 to generate $PbSO_4$, as shown in reaction (2). Thus, after this reaction, both PbO_2 and Pb from the different electrodes have converted into $PbSO_4$. The composition of the product from this step was confirmed by the XRD results, which showed the disappearance of peaks corresponding to Pb and PbO_2, with only signals from $PbSO_4$ remaining in Fig. 1c.

$$PbO_2 + Na_2SO_3 + H_2SO_4 \xrightarrow{H_2O} PbSO_4 + Na_2SO_4 + H_2O \quad (1)$$

$$Pb + H_2SO_4 \xrightarrow{H_2O} PbSO_4 + H_2 \quad (2)$$

Due to the low reactivity of $PbSO_4$, a desulfurization reaction is necessary. To achieve this, excess ammonium carbonate ($(NH_4)_2CO_3$) was added in the second step to react with $PbSO_4$, producing lead carbonate ($PbCO_3$), as shown in reaction (3). XRD results (Fig. 1d) of the product displayed 2θ peaks corresponding to $PbCO_3$, confirming its formation. In addition, energy dispersive spectrometry (EDS) measurements (Fig. S3†) showed the complete disappearance of sulfur from the carbonate product, indicating a successful conversion of $PbSO_4$ to $PbCO_3$.

$$PbSO_4 + (NH_4)_2CO_3 \xrightarrow{H_2O} PbCO_3 + (NH_4)_2SO_4 \quad (3)$$

In the final step, as shown in reaction (4), the lead-based compounds were added to a dilute nitric acid solution, where $PbCO_3$ reacted to form lead nitrate ($Pb(NO_3)_2$). Subsequently, potassium iodide (KI) was added, producing the desired end product lead iodide (PbI_2) as a precipitate. To further enhance the chemical purity of PbI_2, the product was re-crystallized. XRD measurements were then conducted to confirm the composition of the final product, as shown in Fig. 2a, which matches the reference pattern for PbI_2.

$$PbCO_3 \xrightarrow[2)KI]{1)HNO_3,H_2O} PbI_2 \quad (4)$$

It is worth mentioning that we used the mixture of lead compounds originating from both electrodes in the first recovery reaction, which only allows an approximate estimate of the recovery yield. However, due to the limited solubility of these lead compounds in aqueous solution, as summarized in Table S1,† more than 99% of the lead species can be successfully recycled during this initial step, allowing nearly all of the lead compounds to be collected for the production of lead iodide. Moreover, to minimize lead contamination during the recycling process and reduce waste, we also recycled all reaction solutions from the previous steps, repeating the reactions under the same conditions. The same products were obtained, as confirmed by the XRD results shown in Fig. S4.† This approach also effectively mitigates the environmental impact of the other chemicals used.

In addition, we estimated the costs associated with the recycling process to approximately USD 1.3 per gram lead iodide. The details of our estimate can be found in Table S2.† The obtained cost is significantly lower than the commercial price of lead iodide, which exceeds USD 3 per gram lead iodide.

Purity assessment of recycled PbI_2

The quality of PbI_2 is critical for the performance of PSCs. Therefore, we systematically compared the quality of the recycled PbI_2 with that of pure, commercially available PbI_2. The XRD patterns of the pure PbI_2 (Fig. S5a†) showed differences in peak width and peak ratios as compared to the recycled PbI_2, indicating differences in crystallinity, crystal size and possibly preferential crystal orientation. These differences were further confirmed by scanning electron microscopy (SEM) experiments on the two PbI_2 powders, as observed in Fig. S5b and c.† Furthermore, EDS was performed to analyze the chemical elements present and their relative abundances. EDS analyses (Fig. 2b and c) showed only lead and iodine to be present in both samples; with identical ratios, indicating the same material composition. To further investigate the elemental composition at the surface of the PbI_2 films, we employed X-ray photoelectron spectroscopy (XPS). Results from XPS measurements in Fig. 2d and e showed identical peak positions for Pb (4f) and I (3d) in both samples, confirming that the elements in recycled PbI_2 experience the same chemical environment as in the commercial PbI_2. In other words, the recycled PbI_2 exhibits similar purity as the pure, commercially obtainable PbI_2.

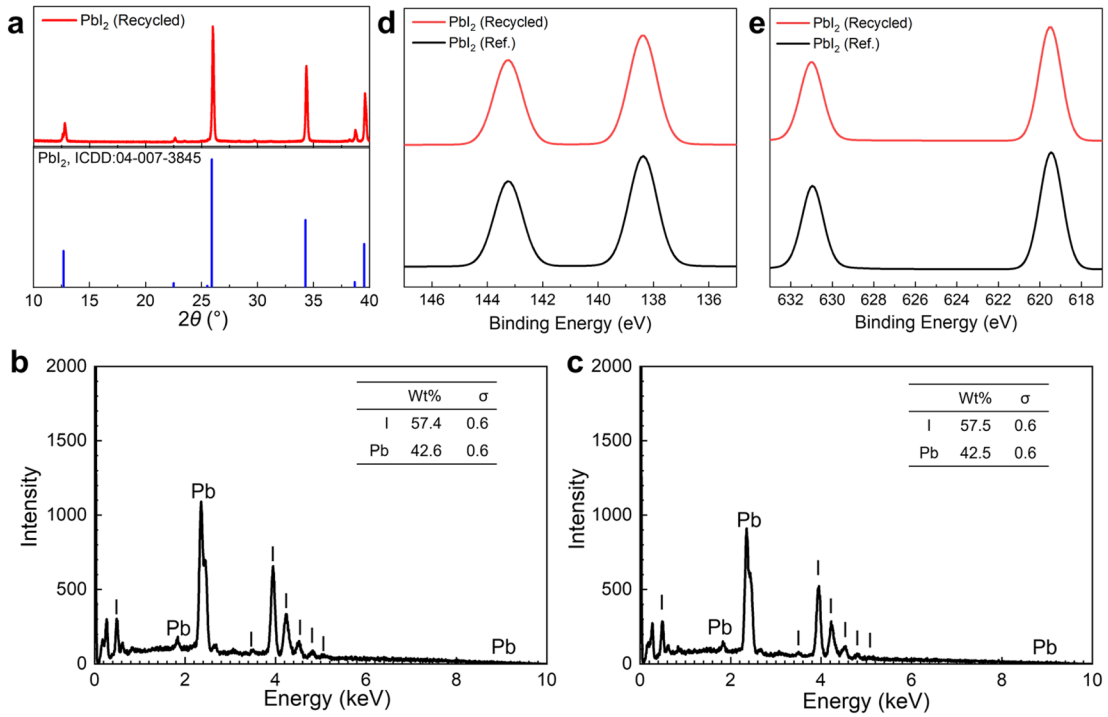

Fig. 2 (a) XRD patterns of recycled PbI_2 and its reference XRD patterns; EDS spectrum of (b) recycled PbI_2 powder and (c) pure, commercially obtainable PbI_2 powder; XPS core level signals of (d) Pb 4f and (e) I 3d of recycled and pure, commercially available PbI_2.

Perovskite film and solar cell fabrication

To assess the quality of recycled PbI_2 for use in PSCs, we selected a formamidinium lead triiodide ($FAPbI_3$) perovskite composition to fabricate perovskite films and subsequent solar cells. XRD results (Fig. 3a) show no presence of PbI_2 or δ-$FAPbI_3$ peaks in the films generated, indicating the formation of a pure α-$FAPbI_3$ phase. Furthermore, comparable ratios of the (001) and (002) XRD peaks in the peaks from the two sources of PbI_2 suggest that both perovskite films exhibited similar crystallization properties.[21] SEM images in Fig. 3b and c show compact, pinhole-free polycrystalline perovskite films with similar grain sizes and surface morphologies, consistent with the XRD

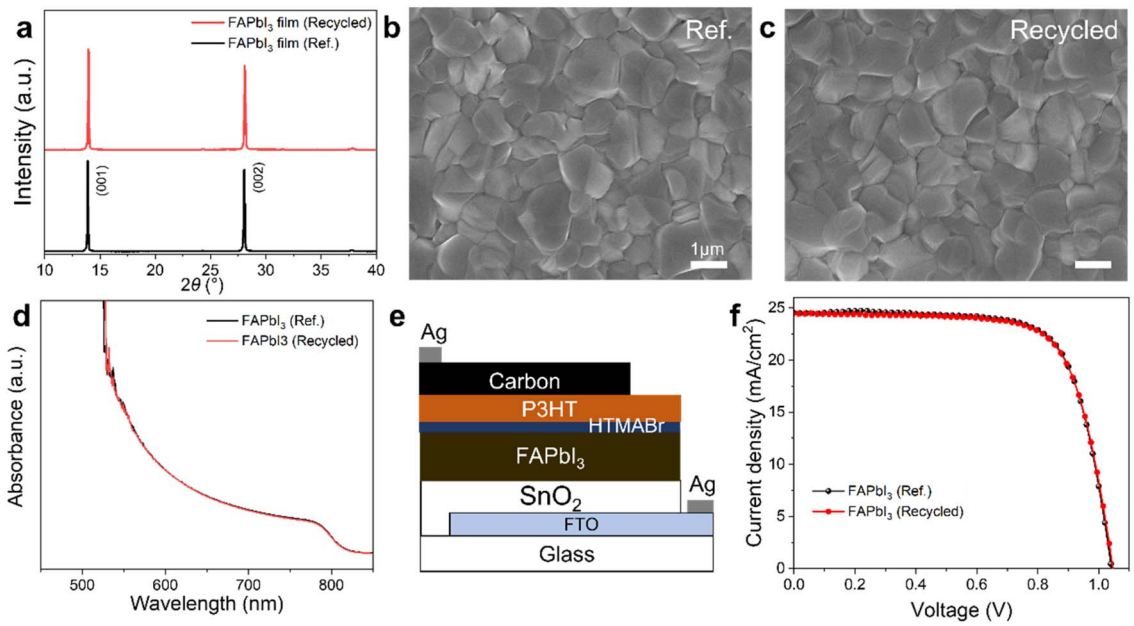

Fig. 3 (a) XRD patterns of $FAPbI_3$ films fabricated from pure, commercially available and recycled PbI_2; SEM images of $FAPbI_3$ films fabricated from (b) commercially obtainable and (c) recycled PbI_2; (d) UV-vis spectra of $FAPbI_3$ films fabricated from commercially available and recycled PbI_2; (e) the architecture of C-PSCs; (f) JV-curve of champion devices fabricated from commercially available and recycled PbI_2.

Table 1 Photovoltaic parameters of champion C-PSCs fabricated from commercially available and recycled PbI_2

	J_{sc} (mA cm^{-2})	V_{oc} (V)	FF	PCE (%)
C-PSCs (ref.)	24.50	1.039	0.725	18.45
C-PSCs (recycled)	24.46	1.042	0.721	18.38

findings. UV-vis spectra (Fig. 3d) further demonstrate that both films display similar light absorption properties.

Lastly, as shown in Fig. 3e, carbon-based PSCs (C-PSCs) with the architecture of fluorine-doped tin oxide coated glass (FTO glass)/tin oxide (SnO_2)/$FAPbI_3$/*n*-hexyl trimethyl ammonium bromide (HTMABr)/P3HT/carbon were fabricated to investigate the effect of recycled PbI_2 on device performance. The *JV*-curve in Fig. 3f shows that the device fabricated with recycled PbI_2 generates a champion power conversion efficiency (PCE) of 18.38%, demonstrating a performance comparable to C-PSCs made from commercially available PbI_2. The parameters of the champion devices are detailed in Table 1. Moreover, statistical box charts for various photovoltaic parameters (photocurrent density (J_{sc}), open-circuit voltage (V_{OC}), fill factor (FF), PCE) from 15 separate devices, as summarized in Fig. S6,† also reveal that PSCs fabricated with recycled PbI_2 exhibit a performance comparable to those made from pure, purchased PbI_2.

Conclusions

Recycling of lead to replace the exploration of new sources is essential for minimizing lead pollution and protecting both the environment and human health. In this study, we have established a straightforward recycling pathway to convert lead compounds from combined positive and negative electrodes of lead–acid batteries into PbI_2, a key component for efficient and stable PSCs. This opens a new circular resource flow pathway for Pb-containing compounds. The recycled PbI_2 was characterized in detail to demonstrate that it meets the required purity standards and comparable quality to commercially available PbI_2. Implementing this recycling strategy will mitigate the environmental impact of toxic lead and promote the future commercialization of perovskite PVs.

Data availability

The data supporting this article have been included as part of the ESI.†

Author contributions

Jiajia Suo: methodology, investigation, writing original draft. Bowen Yang: investigation. Sonja Prideaux: investigation. Henrik Petterson: conceptualization. Lars Kloo: conceptualization, methodology, supervision. All authors read and approved the final manuscript.

Conflicts of interest

Henrik Petterson and Lars Kloo are co-founders of Dyenamo AB.

Acknowledgements

J. Suo, S. Prideaux, H. Petterson and L. Kloo acknowledge the Swedish Energy Agency with project no. P2023-00064. J. Suo, B. Yang and H. Petterson acknowledge the Vinnova with project no. 2023-01428.

References

1 A. Agresti, F. Di Giacomo, S. Pescetelli and A. Di Carlo, *Nano Energy*, 2024, **122**, 109317.
2 L. Zhang, Y. Wang, X. Meng, J. Zhang, P. Wu, M. Wang, F. Cao, C. Chen, Z. Wang, F. Yang, X. Li, Y. Zou, X. Jin, Y. Jiang, H. Li, Y. Liu, T. Bu, B. Yan, Y. Li, J. Fang, L. Xiao, J. Yang, F. Huang, S. Liu, J. Yao, L. Liao, L. Li, F. Zhang, Y. Zhan, Y. Chen, Y. Mai and L. Ding, *Mater. Futures*, 2024, **3**, 022101.
3 B. Yang, J. Suo, E. Mosconi, D. Ricciarelli, W. Tress, F. D. Angelis, H.-S. Kim and A. Hagfeldt, *ACS Energy Lett.*, 2020, **5**, 3159–3167s.
4 B. Yang, J. Suo, D. Bogachuk, W. Kaiser, C. Baretzky, O. Er-Raji, G. Loukeris, A. A. Alothman, E. Mosconi, M. Kohlstädt, U. Würfel, F. De Angelis and A. Hagfeldt, *Energy Environ. Sci.*, 2024, **17**, 1549–1558.
5 J. Suo, B. Yang, E. Mosconi, H.-S. Choi, Y. Kim, S. M. Zakeeruddin, F. De Angelis, M. Grätzel, H.-S. Kim and A. Hagfeldt, *Adv. Funct. Mater.*, 2021, **31**, 2102902.
6 B. Ding, Y. Ding, J. Peng, J. Romano-deGea, L. E. K. Frederiksen, H. Kanda, O. A. Syzgantseva, M. A. Syzgantseva, J.-N. Audinot, J. Bour, S. Zhang, T. Wirtz, Z. Fei, P. Dörflinger, N. Shibayama, Y. Niu, S. Hu, S. Zhang, F. F. Tirani, Y. Liu, G.-J. Yang, K. Brooks, L. Hu, S. Kinge, V. Dyakonov, X. Zhang, S. Dai, P. J. Dyson and M. K. Nazeeruddin, *Nature*, 2024, **628**, 299–305.
7 J. Zhou, L. Tan, Y. Liu, H. Li, X. Liu, M. Li, S. Wang, Y. Zhang, C. Jiang, R. Hua, W. Tress, S. Meloni and C. Yi, *Joule*, 2024, **8**, 1691–1706.
8 H. Chen, C. Liu, J. Xu, A. Maxwell, W. Zhou, Y. Yang, Q. Zhou, A. S. R. Bati, H. Wan, Z. Wang, L. Zeng, J. Wang, P. Serles, Y. Liu, S. Teale, Y. Liu, M. I. Saidaminov, M. Li, N. Rolston, S. Hoogland, T. Filleter, M. G. Kanatzidis, B. Chen, Z. Ning and E. H. Sargent, *Science*, 2024, **384**, 189–193.
9 S. Liu, J. Li, W. Xiao, R. Chen, Z. Sun, Y. Zhang, X. Lei, S. Hu, M. Kober-Czerny, J. Wang, F. Ren, Q. Zhou, H. Raza, Y. Gao, Y. Ji, S. Li, H. Li, L. Qiu, W. Huang, Y. Zhao, B. Xu, Z. Liu, H. J. Snaith, N.-G. Park and W. Chen, *Nature*, 2024, **632**, 536–542.
10 J. Suo, B. Yang, E. Mosconi, D. Bogachuk, T. A. S. Doherty, K. Frohna, D. J. Kubicki, F. Fu, Y. Kim, O. Er-Raji, T. Zhang, L. Baldinelli, L. Wagner, A. N. Tiwari, F. Gao, A. Hinsch, S. D. Stranks, F. De Angelis and A. Hagfeldt, *Nat. Energy*, 2024, **9**, 172–183.

11 R. Azmi, E. Ugur, A. Seitkhan, F. Aljamaan, A. S. Subbiah, J. Liu, G. T. Harrison, M. I. Nugraha, M. K. Eswaran, M. Babics, Y. Chen, F. Xu, T. G. Allen, A. ur Rehman, C.-L. Wang, T. D. Anthopoulos, U. Schwingenschlögl, M. De Bastiani, E. Aydin and S. De Wolf, *Science*, 2022, **378**, 73–77.
12 Z. Shen, Q. Han, X. Luo, Y. Shen, Y. Wang, Y. Yuan, Y. Zhang, Y. Yang and L. Han, *Nat. Photonics*, 2024, **18**, 450–457.
13 P. Zhu, C. Chen, J. Dai, Y. Zhang, R. Mao, S. Chen, J. Huang and J. Zhu, *Adv. Mater.*, 2024, **36**, 2307357.
14 T. D. Siegler, A. Dawson, P. Lobaccaro, D. Ung, M. E. Beck, G. Nilsen and L. L. Tinker, *ACS Energy Lett.*, 2022, **7**, 1728–1734.
15 B. Chen, C. Fei, S. Chen, H. Gu, X. Xiao and J. Huang, *Nat. Commun.*, 2021, **12**, 5859.
16 L. Wagner, J. Suo, B. Yang, D. Bogachuk, E. Gervais, R. Pietzcker, A. Gassmann and J. C. Goldschmidt, *Joule*, 2024, **8**, 1142–1160.
17 P.-Y. Chen, J. Qi, M. T. Klug, X. Dang, P. T. Hammond and A. M. Belcher, *Energy Environ. Sci.*, 2014, **7**, 3659–3665.
18 C. Li, Z. Zhu, Y. Wang, Q. Guo, C. Wang, P. Zhong, Z. Tan and R. Yang, *Nano Energy*, 2020, **69**, 104380.
19 J. Li, C. Duan, L. Yuan, Z. Liu, H. Zhu, J. Ren and K. Yan, *Environ. Sci. Technol.*, 2021, **55**, 8309–8317.
20 L. Xie, Q. Zeng, Q. Li, S. Wang, L. Li, Z. Li, F. Liu, X. Hao and F. Hao, *J. Phys. Chem. Lett.*, 2021, **12**, 9595–9601.
21 J. Suo, B. Yang, J. Jeong, T. Zhang, S. Olthof, F. Gao, M. Grätzel, G. Boschloo and A. Hagfeldt, *Nano Energy*, 2022, **94**, 106924.